MITLibraries | DSpace@MIT

MIT Open Access Articles

Cell Polarity Determinants Establish Asymmetry in MEN Signaling

Massachusetts Institute of Technology

Cell Polarity Determinants Establish Asymmetry in MEN Signaling

Fernando Monje-Casas[1,2] and Angelika Amon[1,*]
[1]David H. Koch Institute for Integrative Cancer Research and Howard Hughes Medical Institute, Massachusetts Institute of Technology, E17-233, 40 Ames Street, Cambridge, MA 02139, USA
[2]Present address: Centro Andaluz de Biología Molecular y Medicina Regenerativa (CABIMER), Avda. Américo Vespucio, s/n, 41092 Sevilla, Spain
*Correspondence: angelika@mit.edu
DOI 10.1016/j.devcel.2008.11.002

SUMMARY

Components of the mitotic exit network (MEN), a signaling pathway that triggers exit from mitosis, localize to the spindle pole body (SPB) that migrates into the daughter cell during anaphase but are largely absent from the SPB that remains in the mother cell. Through the analysis of one of the determinants of this asymmetry, Bfa1, we find that the machinery responsible for establishing cell polarity and cytoplasmic microtubules collaborate to establish MEN asymmetry. In cells defective in the Cdc42 signaling pathway or the formin Bni1, Bfa1 localizes to both SPBs. The quantitative analysis of Bfa1 localization further shows that Bfa1 can associate with both SPBs in a transient and highly dynamic fashion, but the protein is stabilized on the SPB that migrates into the daughter cell during anaphase through microtubule-bud cortex interactions. Our results indicate that mother-daughter cell asymmetry determinants establish MEN signaling asymmetry through microtubule-bud cortex interactions.

INTRODUCTION

In budding yeast, bud formation is initiated as cells enter the cell cycle and is mediated by the polarization of the actin cytoskeleton. The Rho GTPase Cdc42 and its guanine nucleotide exchange factor (GEF) Cdc24 are central to this process (Pruyne and Bretscher, 2000a). Cortical cues that were established during the previous cell cycle cause Cdc42-GTP to accumulate at the site of bud emergence (Park et al., 1997, 1999; Zheng et al., 1995). Cdc42-GTP then recruits the two partially redundant p21-activated kinases (PAKs) Cla4 and Ste20 and activates them (Benton et al., 1997; Leberer et al., 1997; Peter et al., 1996; Vojtek and Cooper, 1995). The 12S polarisome is thought to function as a scaffold for Cdc42 signaling complexes at the plasma membrane and to link Cdc42-PAK signals to the actin cytoskeleton (Evangelista et al., 1997; Fujiwara et al., 1998; Kohno et al., 1996; Sheu et al., 1998). The two formins Bni1 and Bnr1, components of the polarisome, are key factors in promoting actin cytoskeleton polarization. Without formins, actin polymerization is impaired and actin cables are not directed to the site of bud emergence (Buttery et al., 2007; Imamura et al., 1997; Moseley and Goode, 2005). Polarized actin cables transport vesicles into the bud, thereby promoting preferential growth in the bud during early stages of the cell cycle (Pruyne and Bretscher, 2000b). The septin ring, an hourglass-shaped collar at the mother-bud neck, functions as a diffusion barrier, ensuring that the cortical components transported into the bud during bud growth remain localized in the bud (Faty et al., 2002; Longtine and Bi, 2003).

Budding is one of many aspects of the *Saccharomyces cerevisiae* life cycle that requires the asymmetric localization of its components. A signaling pathway known as the mitotic exit network (MEN) is also regulated by the asymmetric localization of its components (McCollum and Gould, 2001; Seshan and Amon, 2004; Stegmeier and Amon, 2004). The MEN promotes exit from mitosis by triggering the release of the protein phosphatase Cdc14 from the nucleolus (Shou et al., 1999; Visintin et al., 1999). This release allows Cdc14 to become active in the nucleus and cytoplasm, where it dephosphorylates its targets to bring about the inactivation of cyclin-dependent kinases (CDKs). This inactivation of mitotic CDKs promotes exit from mitosis (Visintin et al., 1998).

The MEN resembles a RAS-like signaling pathway, with the GTPase Tem1 at the top of the pathway. The GTPase is negatively regulated by the two-component GTPase-activating protein complex (GAP) Bub2-Bfa1 and positively regulated by the putative guanine nucleotide exchange factor (GEF) Lte1 (Stegmeier and Amon, 2004). Bfa1, Bub2, and Tem1 form a complex (henceforth the Tem1 complex) that localizes to spindle pole bodies (SPBs) in an asymmetric manner. During metaphase and anaphase, the complex is found predominantly on the spindle pole that migrates into the bud during anaphase (Bardin et al., 2000; Pereira et al., 2000). Localization of Tem1 at SPBs depends on the Bub2-Bfa1 complex, but the converse is not true (Pereira et al., 2000). Bub2 and Bfa1, however, depend on each other for their localization to SPBs. Lte1 localizes predominantly to the bud, which has led to the proposal that entry of the SPB bearing the Tem1 complex during anaphase causes activation of the mitotic exit pathway (Bardin et al., 2000; Pereira et al., 2000). Consistent with this idea are the observations that the Tem1-GFP signal increases at SPBs during anaphase in a Lte1-dependent manner, and that Cdc15, the protein kinase thought to function downstream of Tem1, is first recruited to the SPB that migrates into the bud during anaphase and only later associates with the SPB that remains in the mother cell (Menssen et al., 2001; Molk et al., 2004).

The mechanism whereby the asymmetric localization of the Tem1 complex is established is not understood. During an unperturbed cell cycle, it is usually the old SPB that migrates into the bud during anaphase and that carries the Tem1 complex. Interfering with this inheritance pattern does not, however, affect the localization pattern of the Tem1 complex (Pereira et al., 2001). The position of the spindle does play a role in establishing MEN asymmetry. In cells where the spindle is not correctly positioned along the mother-bud axis, the Bfa1-Bub2 complex is present on both SPBs (D'Aquino et al., 2005; Pereira and Schiebel, 2005; Pereira et al., 2001). Furthermore, such cells delay exit from mitosis due to activation of the spindle position checkpoint until spindle position has been corrected. How spindle position affects the localization of the Tem1 complex is not known.

Because localization of Tem1 and Bub2 depend on Bfa1, we have investigated the basis for the asymmetric localization of Bfa1. We find that neither migration of the Bfa1-bearing SPB through the bud neck nor the forces acting on SPBs while the spindle is being positioned or elongated are responsible for localizing Bfa1. Instead, our results indicate that cell polarity determinants, which are responsible for establishing the differences between the mother and bud cortex and the interactions of cytoplasmic microtubules with the bud cortex, are essential for establishing Bfa1 asymmetry. The quantitative analysis of Bfa1 localization further showed that Bfa1 associates with both SPBs in a transient fashion, but is stabilized on the SPB that migrates into the daughter pole during anaphase through microtubule-bud cortex interactions. In cells in which the anaphase spindle is mispositioned in that both SPBs are located in the mother cell, Bfa1 is highly dynamic on both SPBs. We propose that microtubule-bud cortex interactions stabilize the Tem1 complex at the SPB that migrates into the bud during anaphase.

RESULTS

Localization of Bfa1 Is Dynamic during the Cell Cycle

To determine how the asymmetry in Tem1 complex localization is established, we examined the localization of an enhanced GFP-tagged version of Bfa1 (Bfa1-eGFP) by live-cell microscopy. This fusion was functional as judged by the ability of cells carrying this allele as the sole source of Bfa1 to arrest in metaphase upon treatment with the microtubule depolymerizing drug nocodazole (data not shown; cells defective in Bfa1 function do not arrest in metaphase in response to nocodazole treatment; Li, 1999).

The localization pattern of the Bfa1-eGFP fusion recapitulated that of a previously described 3HA-Bfa1 fusion and other Tem1 complex components (Bardin et al., 2000; D'Aquino et al., 2005; Pereira et al., 2000) (see Figures S1A and S2 available online). Bfa1-eGFP was found on SPBs in small budded cells (Figure S1B). During metaphase Bfa1-eGFP localized to the SPB destined to migrate into the daughter cell (Figure S1B). However, in contrast to the 3HA-Bfa1 fusion, which is rarely detected on both SPBs, Bfa1-eGFP was also weakly detected on the SPB located distally from the bud neck (mother SPB; mSPB) in a high proportion of cells. Live-cell analysis of Bfa1-eGFP confirmed these results. Bfa1 was localized predominantly on the SPB that was located close to the bud neck, which is also
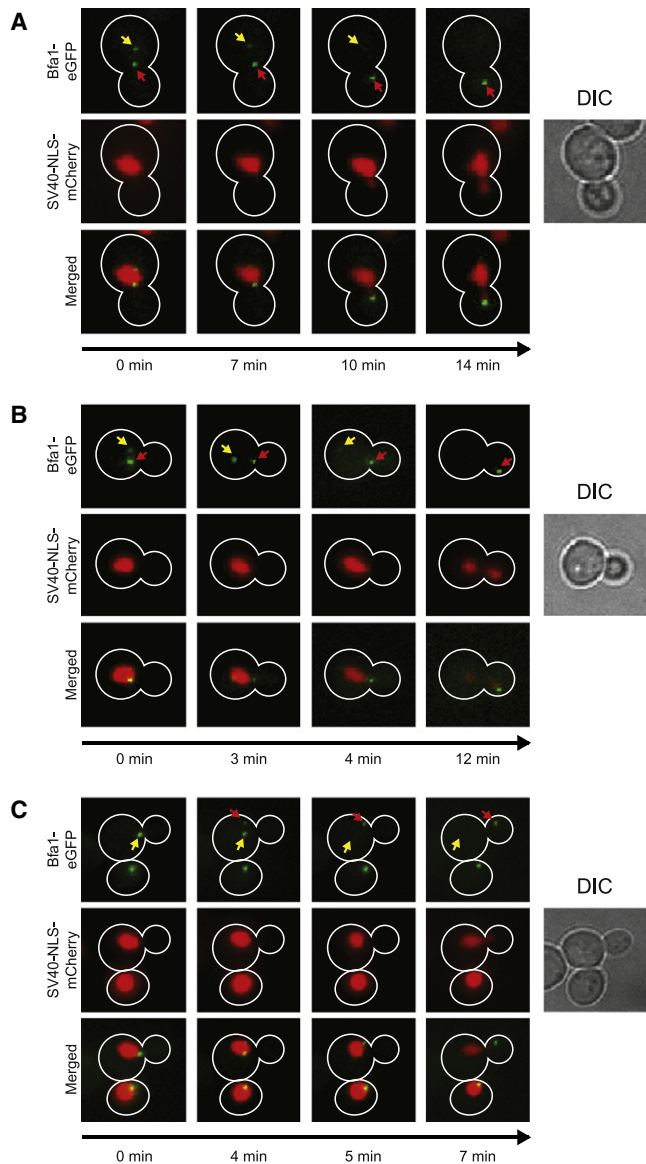

Figure 1. Bfa1 Localization in Live Cells
(A–C) Time-lapse microscopy of live cells carrying Bfa1-eGFP (green) and the mCherry fluorescent protein (red) with the nuclear localization sequence of SV40 as a nuclear marker (A20646). The red and yellow arrows indicate the position of both SPBs in the cell. Elongation (A and B) or rotation (C) of the spindle can be observed by following these arrows. Morphology of the cells is also shown by DIC. The time-lapse movies for (A), (B), and (C) are shown as Movies S1, S2, and S3, respectively.

the SPB that usually migrates into the daughter cell during anaphase (daughter SPB, dSPB; Figures 1A and 1B; Movies S1 and S2). Localization to the other SPB, the mSPB, was usually more dynamic, with the Bfa1-eGFP signal changing in intensity (Figures 1A and 1B; Movies S1 and S2). These changes in intensity, however, did not correlate with the movements of the nucleus while it was being positioned along the mother-bud axis (Movie S2), which argues against Bfa1 localization at SPBs being determined by the forces exerted on SPBs during nuclear positioning.

Bfa1-eGFP localization did, however, correlate with the points of contact that cytoplasmic microtubules made with the cell cortex. In most cells, Bfa1-eGFP was found on the SPB whose microtubules interacted with the bud cortex. Cells with a metaphase spindle perpendicular to the mother-daughter cell axis, which is likely caused by microtubules from both SPBs interacting with the bud cortex, showed a bright Bfa1-eGFP signal on both SPBs (data not shown). In a small number of cells in which the spindle rotated while the nucleus was being positioned in metaphase, the two SPBs changed position with respect to the bud neck (Figure 1C). Interestingly, in such cells, Bfa1-eGFP was first detected on the SPB close to the bud neck, but as the spindle rotated and the microtubules emanating from this SPB began to interact with the mother cell cortex, Bfa1-eGFP was lost from this SPB and now associated with the SPB that migrated into the daughter cell during the ensuing anaphase (Figure 1C; Movie S3). Together, these results indicate that Bfa1 localization can be highly dynamic during metaphase spindle positioning, and they raise the possibility that Bfa1's asymmetric localization is determined by differences between the mother and bud cortex.

During anaphase a strong Bfa1-eGFP signal was observed on the dSPB, but little or no Bfa1-eGFP was detected on the mSPB (Figure S1B). Live-cell analysis revealed two types of spindle movement during anaphase. In most cells, anaphase spindle elongation coincided with the migration of the SPB through the bud neck, with the Bfa1-eGFP signal disappearing on the SPB that remained in the mother cell and increasing on the SPB entering the daughter cell (Figure 1A). In approximately 30% of the cells (n = 36), anaphase spindle elongation was initiated in the mother cell and only later during anaphase did movement of the dSPB into the bud occur (Figure 1B). In these cells too, Bfa1-eGFP was found on the dSPB as soon as spindle elongation occurred (Figure 1B). These results show that during anaphase Bfa1-eGFP localization is strictly asymmetric, with Bfa1 predominantly localizing to the SPB that enters the bud.

Movement of the SPB through the Bud Neck Does Not Affect Bfa1 Localization

A previous report had implicated components of the bud neck (septins) and the morphogenesis checkpoint in contributing to the asymmetric localization of Bfa1 (Fraschini et al., 2006). Our analysis of Bfa1-eGFP in live cells showed that Bfa1 localizes to the bud-bound SPB even before the dSPB is pulled through the bud neck, which suggests that movement of the SPB through the bud neck was not required for the asymmetric localization of Bfa1. Furthermore, in our hands localization of a 3HA-Bfa1 fusion was normal in septin mutants (cdc12-6; Figure 2A, top panels) and in mutants in which the morphogenesis checkpoint is defective (swe1Δ; Figure 2B) or hyperactive (hsl1Δ; Figure 2C). A fraction of swe1Δ mutants and cdc12-6 swe1Δ double mutants, however, exhibited spindle position defects at the restrictive temperature. In such cells, but not cells with a correctly positioned spindle, Bfa1 asymmetry was lost in a high proportion of the cells (Figure 2A). The same results were obtained with the Bfa1-eGFP fusion (data not shown). Our results indicate that the septin ring and the morphogenesis checkpoint are not required for the asymmetric localization of Bfa1.
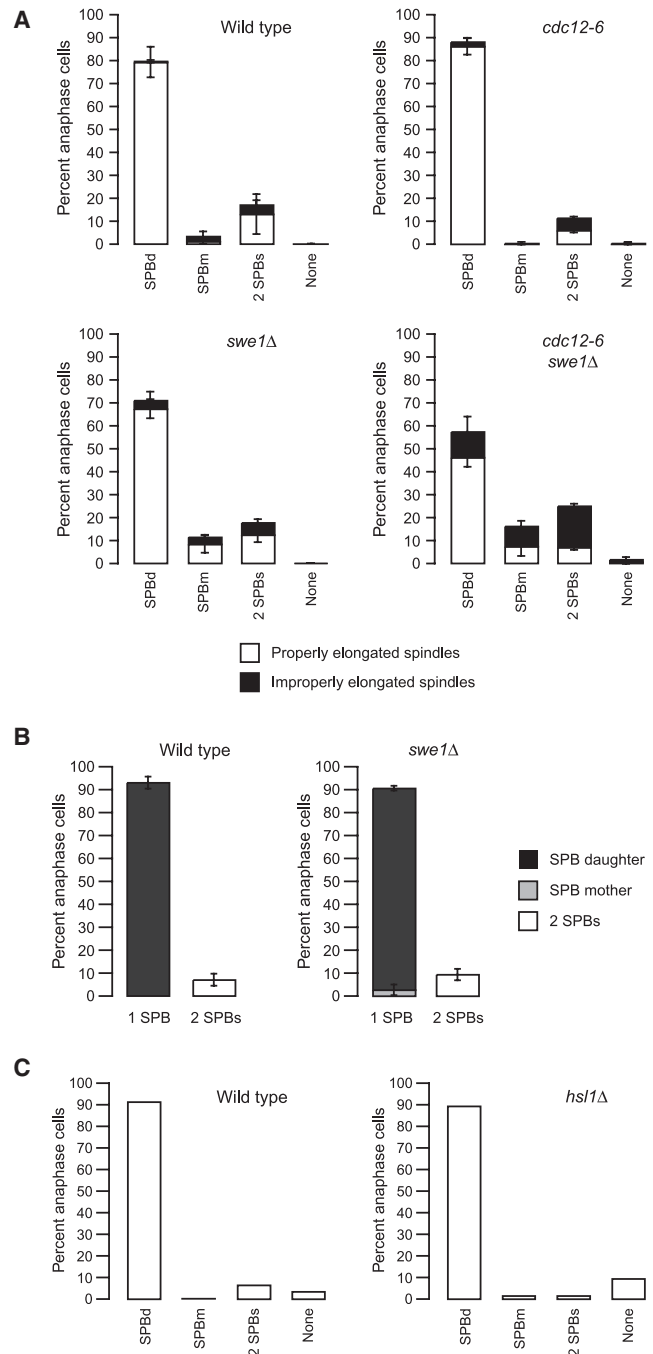

Figure 2. Bfa1 Asymmetry Is Not Dependent on Septins or the Morphogenesis Checkpoint

(A) 3HA-Bfa1 localization in wild-type (A2741), cdc12-6 (A4473), swe1Δ (A20770), and swe1Δ cdc12-6 (A20645) anaphase cells after release from a pheromone-induced arrest into fresh medium at 37°C. Error bars represent the standard deviation (n = 3).

(B) 3HA-Bfa1 localization in wild-type (A2741) and swe1Δ (A20770) anaphase cells after release from a pheromone-induced arrest into fresh media at 25°C. Error bars indicate the standard deviation (n = 3).

(C) 3HA-Bfa1 localization in wild-type (A2741) and hsl1Δ (A19015) anaphase cells after release from a pheromone-induced arrest into fresh media at 25°C.

The Forces Generated during Spindle Elongation Are Not Determinants of Bfa1 Asymmetry

During spindle positioning in metaphase and spindle elongation during anaphase, pulling and pushing forces act on the spindle poles. In particular, the pulling forces exerted on the spindle pole that migrates into the bud during anaphase are greater than those acting on the pole that remains in the mother cell. Although Bfa1 localization did not appear to respond to sudden changes in force during spindle positioning (Figures 1A and 1B; Movies S1 and S2), it was possible that, particularly during anaphase, the asymmetric localization of Bfa1 was dependent on differences in force acting on the two SPBs, with Bfa1 localizing to the SPB experiencing a greater pulling force.

Microtubule motors as well as proteins involved in microtubule capture at the cell cortex play an important role in generating the forces that act on SPBs during spindle positioning (Yeh et al., 2000). Anaphase cells lacking the microtubule motors Dyn1, Kip2, Cin8, or Kar3 or factors important for microtubule capture at the cell cortex Kar9, Num1, Bik1, or Bim1 showed wild-type localization of Bfa1 when the spindle elongated along the mother-bud axis (Figure S3A). However, when the spindle was incorrectly positioned and did not elongate into the bud during anaphase, as it is frequently the case in *kar9Δ* and *dyn1Δ* mutants or in cells lacking *DYN1* and depleted for *KAR9* (*pGAL-URL-KAR9 dyn1Δ*), the majority of cells exhibited very weak Bfa1 localization on both SPBs (Figures S4A, S4B, and S5) (Pereira et al., 2001). Perturbation of microtubule dynamics also affected Bfa1-eGFP localization. Loss of Stu2 leads to fewer and less dynamic cytoplasmic microtubules (Kosco et al., 2001). In a temperature-sensitive *stu2-2* mutant, Bfa1-eGFP was found on both SPBs (Figure S3B). Thus, in cells in which the force distribution on SPBs is altered during anaphase, Bfa1 is localized to both SPBs, raising the possibility that force is indeed a determinant in Bfa1 localization. However, microtubule dynamics and microtubule-cell cortex interactions are also affected in these mutants (Maekawa and Schiebel, 2004; Maekawa et al., 2003). Thus, microtubule-bud cortex interactions and/or mother-bud asymmetry determinants could control Bfa1 localization.

To determine whether forces acting on SPBs localize Bfa1, we examined the consequences of severing spindle or cytoplasmic microtubules. It has been shown previously that microtubules can be severed using a high-energy laser pulse, and that this does not greatly disturb cell integrity (Carvalho and Pellman, 2004). When the spindle midzone was severed during anaphase using laser microsurgery, the forces exerted on both SPBs were transiently perturbed. This was evident by the rapid and erratic movement of microtubules that followed the laser pulse (Movie S4). Bfa1 localization did not change upon severing of the anaphase spindle (Figure 3A; Movie S4; n = 6).

During anaphase B, SPBs are thought to nucleate two to three cytoplasmic microtubules. To simultaneously sever all cytoplasmic microtubules, we chose cells in which only one microtubule bundle was evident. When we severed cytoplasmic microtubules that anchor the SPB in the mother cell, Bfa1 localization was not affected (data not shown; n = 6). However, when we severed the microtubules that anchor the SPB in the bud, we observed a loss of Bfa1 from SPBs in approximately 60% of cells (n = 12; Figure 3B; Movie S5). In 20% of cells Bfa1 reappeared on

SPBs after microtubule repolymerization (n = 12; Figure 3C; Movie S6). Cytoplasmic microtubules reformed (average reformation time = 137.5 ± 47.7 s) in all cells whether or not Bfa1 reassociated with SPBs. This result indicates that SPB-bud cortex interactions alone are not sufficient for Bfa1 to reassociate with SPBs, but suggests that the location where microtubules contact the bud cortex is important for Bfa1 loading. The fact that the formin Bni1, which localizes to the bud tip (Buttery et al., 2007; Ozaki-Kuroda et al., 2001), is required for Bfa1 asymmetry (see below) is consistent with this idea.

Our microtubule-severing studies together with our live-cell analyses indicate that forces exerted on SPBs during spindle position in metaphase and spindle elongation during anaphase are not responsible for the asymmetry in Bfa1 localization. The observation that severing of bud-cortex-interacting cytoplasmic microtubules causes loss of Bfa1 from dSPBs furthermore implicates interactions of cytoplasmic microtubules with the bud cortex in localizing Bfa1-eGFP on dSPBs.

Depolarized Cells Lose Bfa1 Asymmetry

To investigate whether the interactions of microtubules with the bud cortex are important for Bfa1 asymmetry, we first examined the consequences of depolarizing the actin cytoskeleton by expressing a stabilized version of the B-type cyclin Clb2 (Clb2dbΔ). When Clb2dbΔ is overexpressed during a pheromone-induced G1 arrest, cells will, upon release from the block, not bud or form a septin ring (Figure 4D) but progress through the cell cycle and arrest in anaphase (Amon et al., 1994). In approximately 50% of the unbudded cells, 3HA-Bfa1 was present on only one SPB, but in the other half of the population, Bfa1 localized to both SPBs (Figure 4A). This result raised the possibility that in the fraction of cells in which Bfa1 localized to both SPBs mother-daughter asymmetry was lost, but in the fraction of cells in which Bfa1 was asymmetric some mother-daughter asymmetry was maintained. To test this possibility, we correlated Bfa1 localization with cell morphology. Cells that exhibited a rounded morphology showed Bfa1-eGFP association with both SPBs (Figure 4B). The cells that had formed a mating projection during the arrest exhibited Bfa1 asymmetry. Bfa1-eGFP was found on the SPB closer to the protrusion (Figure 4B). The asymmetry in cell morphology indeed reflected polarization of the actin cytoskeleton (Figure 4C). Thus, asymmetry in Bfa1 localization correlates with actin polarization.

Cell Polarity Determinants Are Required for Bfa1 Localization to dSPBs

The observation that depolarization of the actin cytoskeleton correlated with a loss of Bfa1 asymmetry led us to examine the role of the Cdc42 signaling network in Bfa1 asymmetry. The effects of inactivating *CDC42* on Bfa1 localization were striking. In the majority of temperature-sensitive *cdc42-6* cells, Bfa1-eGFP was found on both SPBs (Figure 5A). Inactivation of the Cdc42 effector Cla4 also led to a loss in Bfa1 asymmetry, although the effects were not as severe (Figure 5B), likely because Cla4 and Ste20 functions are partially redundant (Cvrckova et al., 1995).

An intact actin cytoskeleton was also needed to establish the asymmetric localization of Bfa1. Treatment of cells with the actin-depolymerizing drug Latrunculin-A (Lat-A) affected Bfa1
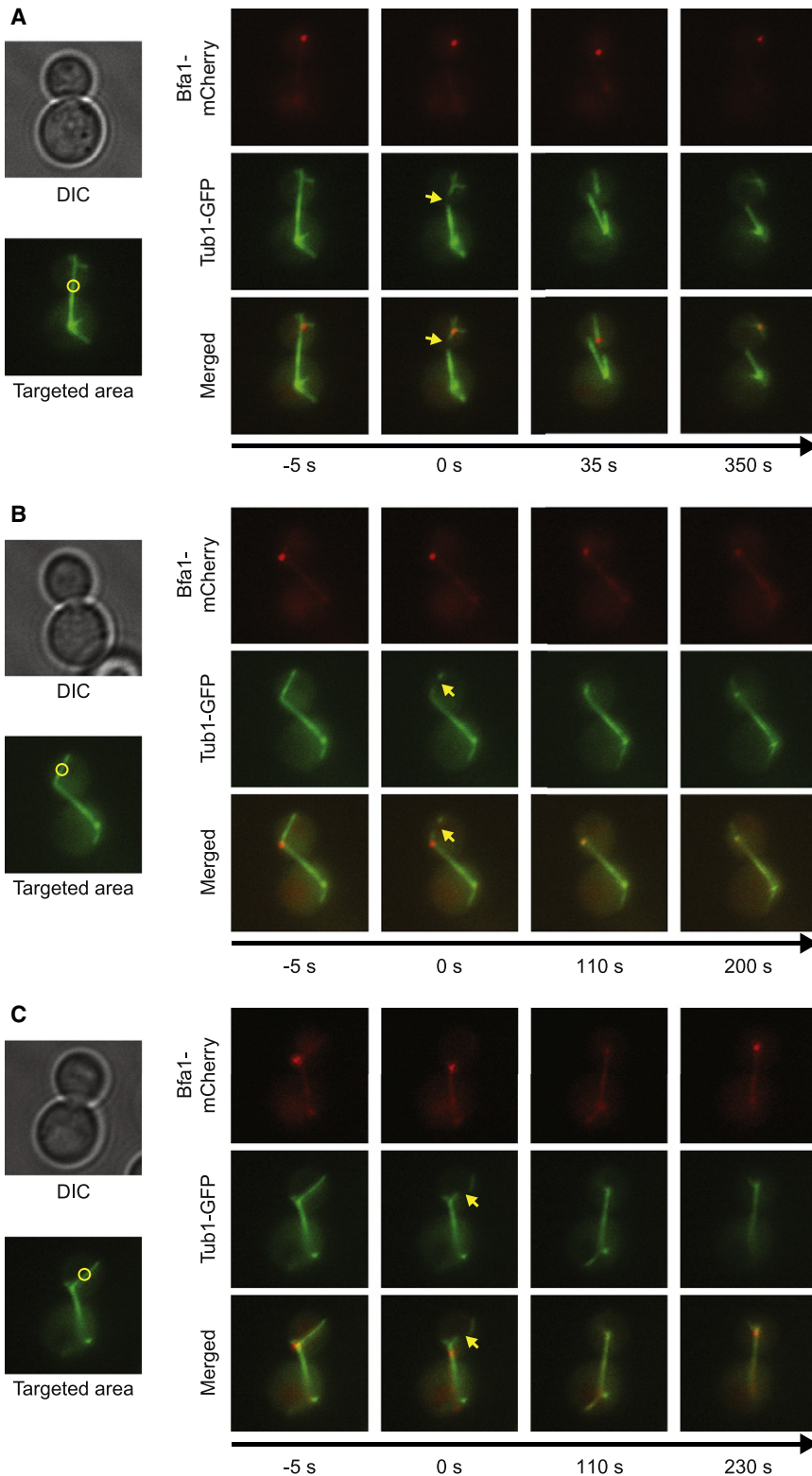
Figure 3. Effects of Microtubule Severing on Bfa1 Localization

Time-lapse microscopy of live cells carrying Bfa1-mCherry (red) and Tub1-GFP (green) fusions (A20648). A pulse of high-energy laser was applied at t = 0 min to sever the spindle ([A]; Movie S4) or cytoplasmic microtubules ([B and C]; Movies S5 and S6). The yellow arrow indicates the site targeted with the laser beam. Morphology of the cells is shown by DIC.

morphogenesis checkpoint; McMillan et al., 1998). In more than 80% of such cells, Bfa1 was found on both SPBs (Figure 5C; Figure S6A). When Lat-A was added at the time of bud formation (40 min after release from the G1 arrest), the percentage of anaphase cells with Bfa1 on both SPBs decreased to 60% (Figure 5C; Figure S6B). Finally, when Lat-A was added to *swe1Δ* cells released from a nocodazole-induced metaphase arrest, Bfa1 localization was not affected (Figure 5C; Figure S6C). Our results indicate that the Cdc42 pathway and the actin cytoskeleton are needed to establish the asymmetry in Bfa1 localization, but they are not needed for maintenance of this asymmetry.

The formins Bni1 and Bnr1 are important for actin cable formation. Deletion of either gene does not affect viability, but deletion of both is lethal (Vallen et al., 2000). Cells carrying a deletion in *BNR1* and the temperature sensitive *bni1-1* allele failed to form a bud after release from a pheromone-induced G1 arrest (Evangelista et al., 2002), but cells progressed through the cell cycle. As in cells expressing Clb2dbΔ, two populations of cells were observed (Figure 5D). In round cells with no sign of polarization, Bfa1 was located at both SPBs. In cells that carried a protrusion (in this case a defective bud, presumably due to incomplete inactivation of Bni1 at the restrictive temperature) and a polarized actin cytoskeleton, Bfa1 localized to one SPB, usually the one closer to the protrusion (Figures 5D and 5E). To determine the contribution of each formin in establishing Bfa1 asymmetry, we also examined Bfa1 localization in each single mutant. Deletion of *BNR1* did not alter

localization. When Lat-A was added immediately (5 min) after release from a pheromone-induced G1 arrest, the cells did not form a bud but proceeded to anaphase (we used a *swe1Δ* mutant to avoid cell cycle arrest due to activation of the the localization pattern of Bfa1 to the SPBs, but Bfa1 was localized to both SPBs in the *bni1-1* mutant that failed to form a bud (Figure 5F). Our results indicate that *BNI1* is required for establishing Bfa1 asymmetry.
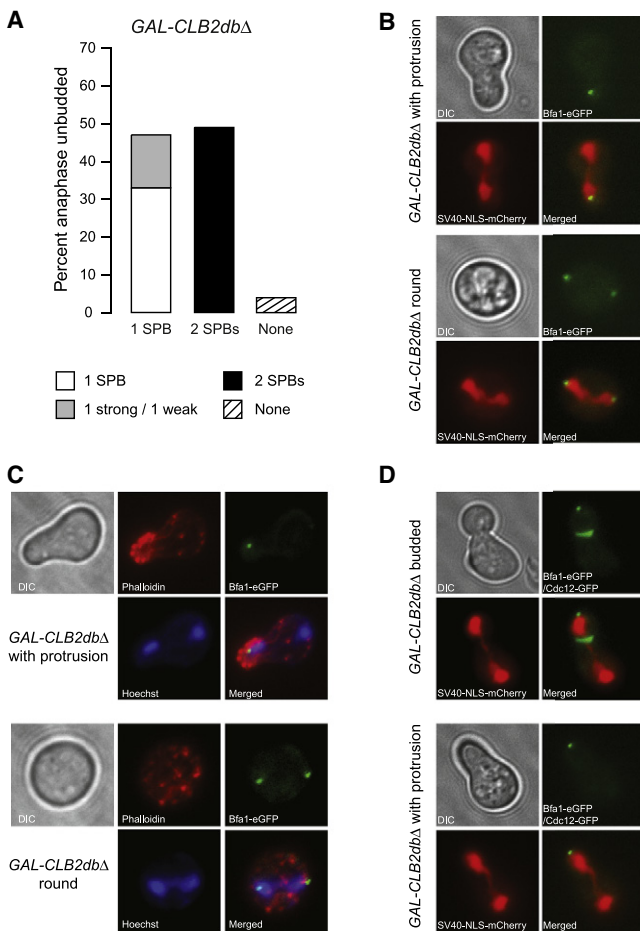
Figure 4. Bfa1 Localization in Cells Overexpressing a Stable Version of Clb2

Cells carrying *CLB2dbΔ* under control of the *GAL1-10* promoter were arrested in G1 with pheromone, treated with 2% galactose for 30 min, and released into media containing 2% galactose.

(A) Localization of Bfa1 is shown in unbudded cells with anaphase spindles also carrying a *3HA-BFA1* fusion (A4379).

(B) DIC images showing the different morphologies observed for unbudded cells overexpressing *CLB2dbΔ*. In this case, the cells carry a Bfa1-eGFP fusion (green) and the mCherry-SV40NLS fusion protein (red; A20647).

(C) Phalloidin staining (red) of unbudded *GAL-CLB2dbΔ* cells carrying Bfa1-eGFP (green) fusions (A20653) after *CLB2dbΔ* overexpression.

(D) *GAL-CLB2dbΔ* cells carrying Cdc12-GFP (green), Bfa1-eGFP (green), and the mCherry-SV40NLS fusion protein (red; A20755).

Bfa1 Loading onto SPBs Occurs after Cell Cycle Entry and Does Not Require Microtubules

Our results indicate that the asymmetry in Bfa1 localization depends on factors involved in actin polarization and on microtubule-cortex interactions. We therefore examined whether the association of Bfa1 with SPBs depended on microtubules. Previous studies demonstrated that depolymerization of microtubules does not affect Bfa1 localization, indicating that microtubules are not needed for maintaining the protein on SPBs (Pereira et al., 2000). To determine whether the initial loading of Bfa1 onto SPBs required microtubules, we placed the sole copy of *BFA1* tagged with GFP under the control of the galactose-inducible *GAL1-10* promoter. Cells arrested in G1 with

pheromone did not load Bfa1 onto SPBs after galactose addition, irrespective of whether microtubules were intact or not (Figure 6A). This result indicates that Bfa1 loading must occur after cells commit to cell cycle entry.

To determine whether microtubules were needed after G1 to load Bfa1 onto SPBs, cells carrying the p*GAL-BFA1* fusion were released from the G1 arrest into medium containing or lacking nocodazole and 30 min later Bfa1-GFP production was induced. Bfa1 loaded onto SPBs within 15 min of galactose addition and with the same kinetics under both conditions (Figure 6B; data not shown). These results show that Bfa1 loading and maintenance on SPBs can occur in the absence of microtubules.

Wild-Type Levels of Bfa1 Association with SPBs Depend on Microtubule-Cortex Interactions

All our results indicate that actin polarity determinants and hence factors important for establishing mother-daughter asymmetry and microtubule-cortex interactions are important for the asymmetric localization of Bfa1. However, our results also indicate that microtubules are not required for Bfa1 association with SPBs, because the protein is present on the poles in nocodazole-treated cells. To resolve this inconsistency, we examined the intensity of Bfa1 signal in cells in which microtubule-cortex interactions as well as microtubule polymerization were defective.

In cells lacking *KAR9* in which the nucleus is mispositioned, cytoplasmic microtubules are directed to the cortex of the mother and the daughter cell with the same frequency (Yeh et al., 2000). In these cells, the Bfa1-eGFP signal was present on both SPBs, but the signal was significantly weaker than in wild-type cells and *kar9Δ* mutants in which the anaphase spindle was positioned correctly (Figure 7A). This was not due to limiting amounts of Bfa1, because in cells lacking formins, in which Bfa1 also localizes to both SPBs, similar amounts of Bfa1 were present (data not shown) and the signal on SPBs was the same or even stronger than in wild-type cells (Figure 7B). These results suggest that microtubule-bud cortex interactions are important for full Bfa1 loading onto SPBs.

In nocodazole-treated cells the Bfa1 signal was not decreased (Figure 6C). However, the depolymerization of microtubules due to nocodazole treatment leads to SPBs positioned side by side so that they can appear as one. The quantification therefore likely reflects the signal generated by two SPBs rather than one and suggests that Bfa1 loading in nocodazole-treated cells is reduced to a similar degree as in cells lacking *KAR9*. Indeed, when metaphase-arrested *cdc23-1* cells were treated with nocodazole, the SPBs did not immediately adopt a side-by-side configuration and the two SPBs could be detected (30 min after nocodazole addition). In these cells the Bfa1-eGFP signal was 30% lower in nocodazole-treated than in untreated cells (Figure 6D). Bfa1 levels at SPBs also diminished when the GFP signal is followed in real time after nocodazole addition and before the SPBs collapse (see Caydasi and Pereira, 2009 [this issue of *Developmental Cell*]). We conclude that microtubules are required for wild-type levels of Bfa1 at SPBs.

The Association of Bfa1 with SPBs Is Dynamic

To further investigate the relationship between microtubule-cortex interactions and Bfa1 localization, we utilized fluorescence recovery after photobleaching (FRAP) to assess the
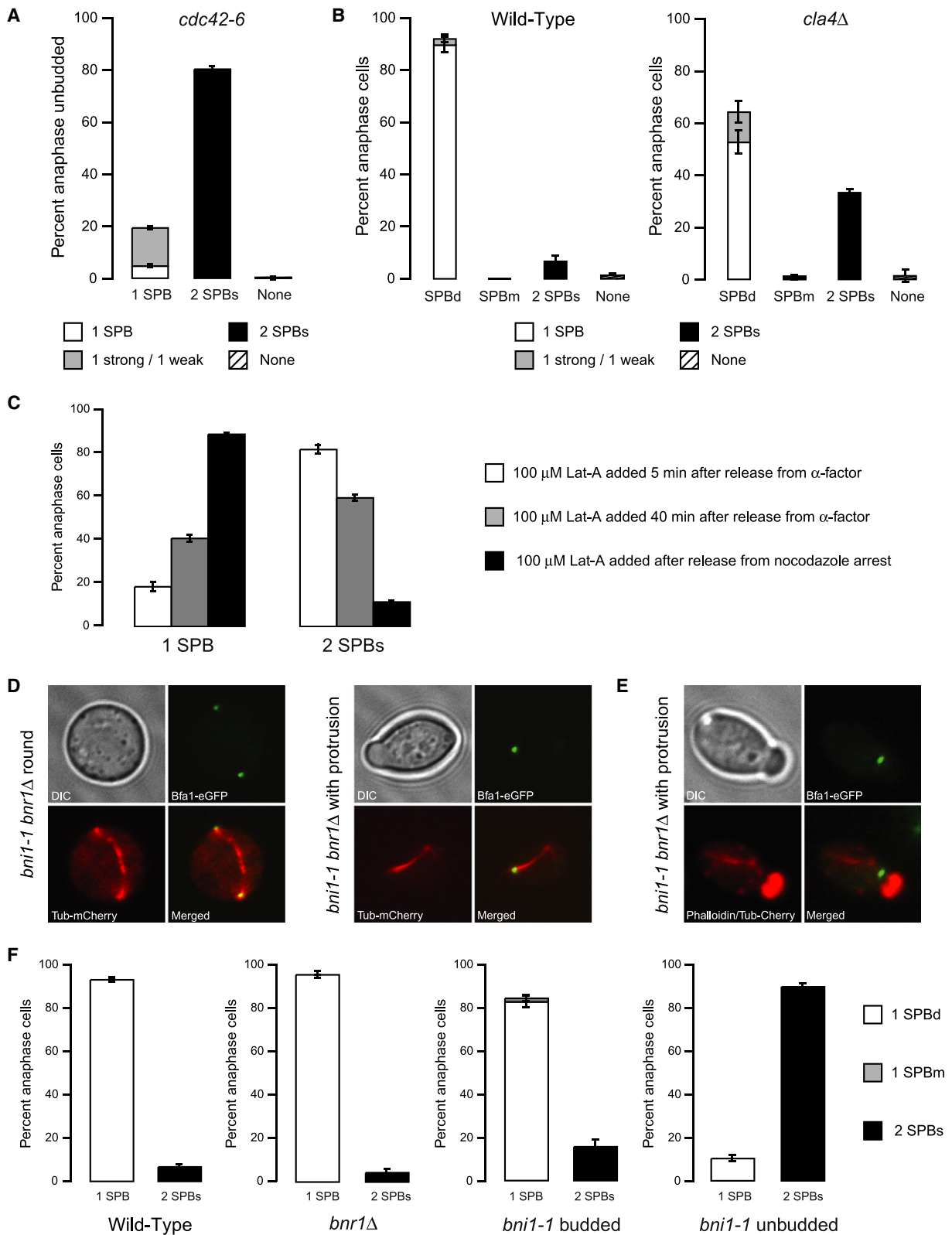
Figure 5. Polarization of the Actin Cytoskeleton Is Needed for Bfa1's Asymmetric Localization

(A and B) Quantification of Bfa1-eGFP localization in (A) unbudded *cdc42-6* (A20655) cells with anaphase spindles after pheromone-induced arrest and release into YPD medium at 37°C, and in (B) wild-type (A20644) and *cla4Δ* (A20654) anaphase cells in YPD at 25°C. Error bars represent standard deviations (n = 3).
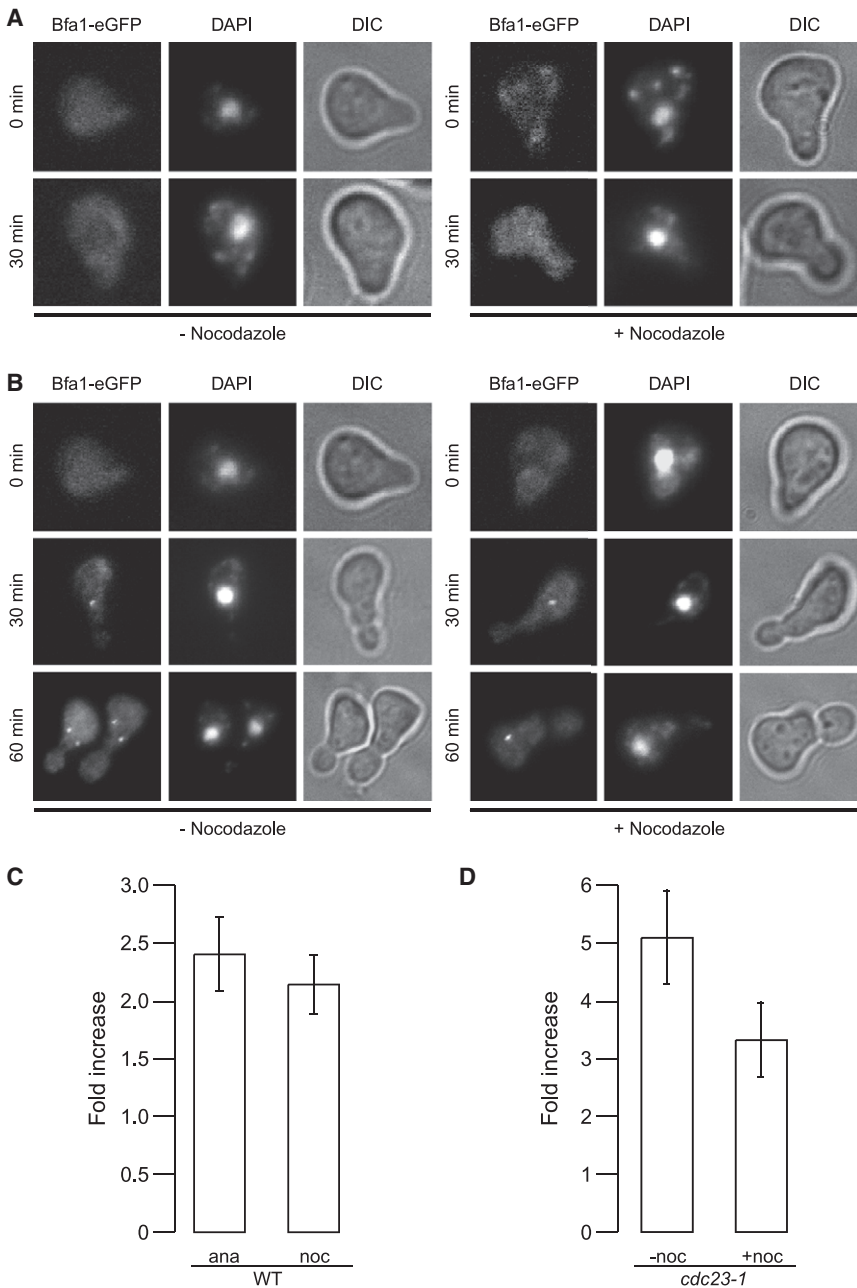
A

| Bfa1-eGFP | DAPI | DIC | | Bfa1-eGFP | DAPI | DIC |

- Nocodazole   + Nocodazole

B

| Bfa1-eGFP | DAPI | DIC | | Bfa1-eGFP | DAPI | DIC |

- Nocodazole   + Nocodazole

C

D

Figure 6. Bfa1 Loading onto SPBs Does Not Require Microtubules and Occurs after Cell Cycle Entry

(A and B) Cells carrying the sole copy of *BFA1-GFP* under the control of the *GAL1-10* promoter (A3487) were arrested in YEP medium containing raffinose in G1 using pheromone. DIC, Bfa1-GFP, and DAPI images are shown. (A) Following 2.5 hr in the pheromone arrest, 15 μg/ml nocodazole or 1% DMSO (mock) was added to the medium, and 30 min later 2% galactose was also added to both cultures. (B) Cells were released into medium containing 15 μg/ml nocodazole or 1% DMSO (mock), and 30 min after the release 2% galactose was added to both cultures.

(C) Wild-type cells carrying a Bfa1-eGFP fusion (A20644) were grown for 3 hr in the presence (noc) or absence of 15 μg/ml nocodazole at 25°C. GFP fluorescence intensity relative to background (cytoplasmic fluorescence signal) was quantified. Error bars represent standard deviations (n = 10). Note that the experiment was performed in parallel with that shown in Figure 7A, and the wild-type control is the same in both cases.

(D) Cells of a *cdc23-1* mutant carrying a Bfa1-eGFP fusion (A21060) were grown for 3 hr at 37°C. Once the cells were arrested in metaphase, 15 μg/ml nocodazole (+noc) or 1% DMSO (−noc) was added and the GFP fluorescence intensity relative to background (cytoplasmic fluorescence signal) was quantified 30 min thereafter. Only cells in which both SPBs were visible were examined. Error bars represent the standard deviations (n = 10).

dynamicity of Bfa1 on SPBs. First, we measured the residence time of Bfa1 in wild-type metaphase cells and distinguished between the SPB that was close to the bud neck (dSPB) and the SPB that was further away from the bud neck (mSPB). To exclude effects of SPB damage on Bfa1 residence time, we

only included measurements where a Bfa1 signal was recovered. When fitted to a single exponential curve, the half recovery time for the Bfa1-eGFP signal was similar for both SPBs (42.85 ± 3.71 and 32.7 ± 4.23; Figure 7C). The percent signal that was recovered differed, however, significantly between the two SPBs (Figure 7D). Seventy percent of the signal was recovered on the mSPB, whereas only 15% was recovered on the dSPB. This result shows that Bfa1 is highly dynamic on the mSPB. In contrast, on the dSPB the majority of Bfa1 is stable (discussed in more detail below).

In nocodazole-treated cells the half recovery time was substantially decreased (12.67 ± 2.02) compared to metaphase
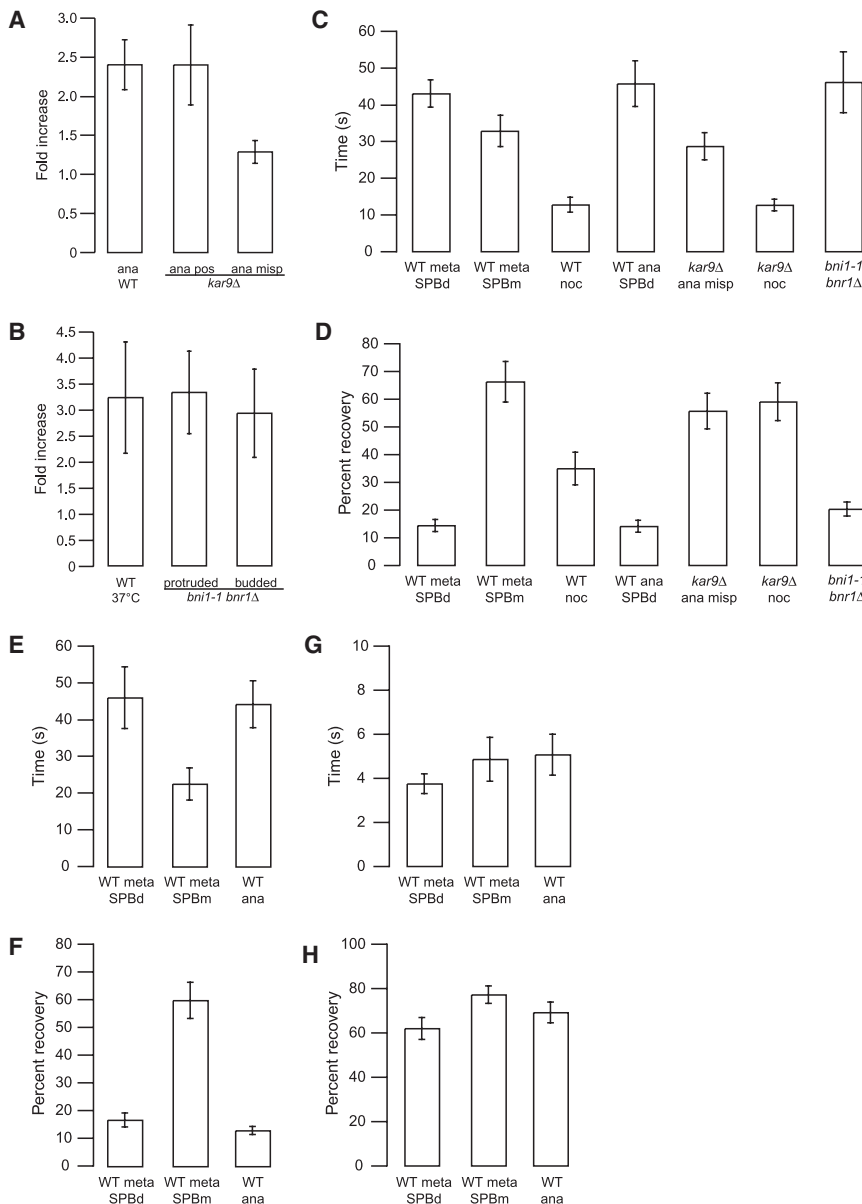
Figure 7. Bfa1 Localization on SPBs Is Dynamic

(A) GFP fluorescence intensity relative to background (cytoplasmic fluorescence signal) was quantified in anaphase (ana) for wild-type (A20644) and *kar9Δ* (A20649) cells with correctly positioned (pos) or mispositioned (misp) spindles after growth for 3hr at 37°C. Error bars represent the standard deviation (n = 10). Note that the experiment was performed in parallel with that shown in Figure 6C, and the wild-type control is the same in both cases.

(B) Quantification of GFP fluorescence intensity relative to background (cytoplasmic fluorescence signal) for anaphase cells of wild-type (A20644) and a double formin mutant (A20652) grown at 37°C for 3 hr. Error bars represent the standard deviation (n = 10).

(C and D) FRAP of the Bfa1-eGFP signal for wild-type (A20644) cells in metaphase (meta) or anaphase (ana), for anaphase *kar9Δ* (A20649) cells with mispositioned (misp) spindles, and in *bni1-1 bnr1Δ* (A20652) anaphase cells. Cells were grown in the absence or presence (noc) of 15 μg/ml nocodazole at 25°C. *bni1-1 bnr1Δ* (A20652) anaphase cells were grown at 37°C. In metaphase cells a distinction was made between the SPB of the mother (SPBm) or the daughter (SPBd) cells. Half-recovery times (C) and the percentages of recovery (D) of the Bfa1-eGFP signal are shown. The error bars represent the standard error of the mean (n = 8).

(E–H) FRAP of the GFP signal in metaphase (meta) or anaphase (ana) wild-type cells carrying Bub2-eGFP ([E and F]; A21088) or Tem1-eGFP ([G and H]; A21089) fusions. The SPBs of the mother (SPBm) or the daughter (SPBd) cells were distinguished in metaphase. Half-recovery times (E and G) and the percentages of recovery (F and H) of the Bub2-eGFP (E and F) and Tem1-eGFP (G and H) signals are shown. The error bars represent the standard error of the mean (n = 8).

cells with an intact microtubule cytoskeleton (Figures 7C and 7D). This indicates that microtubules are required either to lower the on-rate of Bfa1 or for the stabilization of Bfa1 on SPBs. Next we examined the dynamics of Bfa1 in cells in which the spindle was mispositioned. In *kar9Δ* cells the half recovery time for Bfa1-eGFP was significantly shorter than in wild-type anaphase cells with correctly positioned spindles (Figures 7C and 7D). The Bfa1-SPB interaction was, however, more stable than in wild-type cells treated with nocodazole. When microtubules were depolymerized in *kar9Δ* anaphase cells with mispositioned spindles by addition of nocodazole, the half recovery time dropped to the same value that was observed in wild-type cells treated with nocodazole (Figures 7C and 7D), indicating that the dynamicity of Bfa1 increases with the severity of the microtubule disruption. Our results indicate that microtubule-cortex interactions are required for the stable association of Bfa1 with SPBs.

Stabilization of Bfa1 on the Daughter-Bound SPB

The comparison of half-time of recovery of Bfa1 between the SPB that located near the bud neck with that of Bfa1 on the SPB that was located further away from the bud neck revealed no substantial difference (Figure 7C). However, the percentage of recovery was significantly different. Only 15% of the Bfa1 signal was recovered on the dSPB, whereas almost 70% of the Bfa1 signal was recovered on the mSPB (Figure 7D). This was not due to limiting amounts of Bfa1 present in cells, because a similar recovery was seen in cells overexpressing Bfa1 (data not shown). To ensure that the low recovery of signal on the dSPB reflects low mobility of Bfa1 on this SPB rather than photobleaching during image acquisition, we performed a FRAP analysis in which only one final image was acquired 5 min after the laser pulse (Molk et al., 2004). The percentage of Bfa1-eGFP signal recovered was similar to that obtained in experiments

where cells were continuously imaged (13.09 ± 2.61 s), indicating that the low amount of signal recovered on the dSPB was not due to photobleaching.

To demonstrate that the Bfa1-eGFP signal recovered on dSPBs indeed represented a small dynamic pool, we examined Bfa1 dynamicity in pheromone arrested cells. In these cells Bfa1 expressed from the *GAL1-10* promoter fails to load onto SPBs (Figure 6A). Thus, the Bfa1 present on SPBs in G1 should be highly stable. Indeed, Bfa1 was not recovered on SPBs after photobleaching in alpha factor-arrested cells (data not shown). Furthermore, no signal was recovered in FRAP analysis of the integral SPB component Spc42 (data not shown). Together, these results indicate that at least two modes of Bfa1 association with the dSPB exist, whereas only one exists for the mSPB. On the dSPB a small pool of Bfa1 is highly dynamic, comparable to that seen of Bfa1 on mSPB, but the majority of Bfa1 is less dynamic. We conclude that Bfa1 asymmetry is generated via a daughter cell cortex specific loading mechanism.

Microtubules nucleated by the mSPB mostly interact with the mother cell cortex, whereas those nucleated by the dSPB interact with the daughter cell cortex. To determine whether the site of microtubule contact (mother versus daughter cell cortex) determined the stability of the SPB-Bfa1 interaction, we examined Bfa1 dynamics in *kar9Δ* and *bni1-1 bnr1Δ* mutants. In *kar9Δ* cells with mispositioned spindles, cytoplasmic microtubules from both SPBs interact mostly with the mother cell cortex (Yeh et al., 2000). In *bni1-1 bnr1Δ* mutants the entire cell cortex adopts a bud-cortex identity as judged by the finding that Kar9, which normally only localizes to the dSPB, localizes to both SPBs (Sagot et al., 2002). The residence time of Bfa1 on both SPBs of *kar9Δ* cells with mispositioned spindles was similar to that of Bfa1 on mSPBs during metaphase. In *bni1-1 bnr1Δ* mutants the dynamics of Bfa1 on both SPBs was similar to that of Bfa1 on dSPBs during metaphase (half recovery time = 45.97 ± 8.27; percent recovery = 20.24 ± 2.52; Figures 7C and 7D). Our results indicate that cortex identity determines Bfa1 stability on SPBs; SPBs whose microtubules interact with the mother cell cortex cannot stably maintain Bfa1, whereas SPBs whose microtubules interact with the bud cortex can.

Tem1 Mobility Differs from That of the Bub2-Bfa1 Complex

To determine whether Bub2 and Tem1 behave similarly to Bfa1, we examined the dynamics of the two proteins by FRAP. Bub2-eGFP behaved like Bfa1-eGFP. The protein was largely immobile on the dSPB but highly mobile on the mSPB (Figures 7E and 7F).

The dynamicity of Tem1, however, did not resemble that of the Bub2-Bfa1 complex. As observed previously (Molk et al., 2004) Tem1 was highly mobile on both SPBs, and no difference between mSPB and dSPB was observed (Figures 7G and 7H). Between 60% and 80% of the total signal was recovered. The half-recovery time was 4 s. The asymmetry of Tem1 association with SPBs must therefore be a function of the amount of Bub2-Bfa1 complex present on SPBs. Our results indicate that the Bfa1-Bub2 complex is the determinant of Tem1 complex asymmetry that is brought about by cytoplasmic microtubule-mediated cell cortex differences.

DISCUSSION

Spatial Control of Tem1 Complex Localization

The analysis of a Bfa1-eGFP fusion showed that Bfa1 is predominantly found on the SPB whose cytoplasmic microtubules contact the daughter cell cortex. This asymmetry is established during metaphase and becomes more pronounced during anaphase, when the dSPB migrates into the bud. Bub2 shows the same localization pattern and dynamicity as Bfa1, indicating that the two proteins are coregulated. The localization of Bfa1-eGFP is also very similar to that observed previously for Tem1-GFP (Molk et al., 2004; this study). However, the residence time on SPBs differs significantly between the two proteins. On the dSPB, the majority of Bfa1-eGFP is highly stable and only a small pool exhibits dynamicity, while the Tem1-eGFP signal is highly dynamic. We speculate that Bfa1 functions as an anchor for Tem1 on SPBs and that the association of Tem1 with Bfa1-Bub2 provides an additional way of regulating Tem1 complex function.

Several mechanisms could cause Bfa1 to exhibit higher affinity to the SPB that migrates into the daughter cell during anaphase: (1) SPB age and inheritance pattern; (2) movement of the SPB through the bud neck; (3) differential forces acting on the two SPBs; and (4) differences between the mother and bud cortex that, through cytoplasmic microtubules, are conveyed to SPBs. Studies by Pereira et al. (2001) excluded possibility (1). Several lines of evidence also argue against movement of one SPB through the bud neck in directing Bfa1 asymmetry. Our live-cell analysis shows that in a number of cells Bfa1-eGFP asymmetry was generated before the SPB moved through the bud neck. Furthermore, neither a functional septin ring nor an active morphogenesis checkpoint was required for the preferential localization of Bfa1 to the dSPB. Finally, Bfa1 was also present on only one SPB in cells that failed to form a bud neck but where nevertheless polarized.

We also tested whether forces acting on SPBs determine Bfa1 asymmetry. This idea was attractive because during anaphase the dSPB is subjected to a greater pulling force than the mSPB and Bfa1 is almost exclusively localized to this SPB. During spindle positioning in metaphase, both SPBs are subjected to pulling forces, and Bfa1 asymmetry is not as pronounced as in anaphase. However, several lines of evidence argue against force as the source of Bfa1 asymmetry. The SPBs undergo rapid movements while the nucleus is being positioned during metaphase, which did not correlate with changes in Bfa1 localization. More importantly, severing of the anaphase spindle or of cytoplasmic microtubules emanating from the mSPB, which changes the force distribution on SPBs, did not affect Bfa1 localization.

Our studies revealed that actin polarity determinants and microtubule-bud cortex interactions are needed for the stable association of Bfa1 with the dSPB. Mutants in which cell polarity was eliminated or cells lacking an intact actin cytoskeleton exhibited Bfa1 localization on both SPBs. The observation that Bfa1 localization was normal in septin mutants, in which the actin ring is defective but actin cables remain polarized (Jeong et al., 2001; Norden et al., 2004), indicates that it is actin cables that mediate the Tem1 complex asymmetry. Actin cable polarization could be needed for the initial loading of factors that regulate the asymmetric localization of the Bfa1-Bub2 complex, but not for

maintenance of these proteins in the bud cortex. A similar mechanism has been observed for the factors that participate in the positioning of the spindle (Theesfeld et al., 1999), which depends on actin cables early in the cell cycle but becomes actin-independent later on.

In addition to actin polarization, our live-cell analyses demonstrated a correlation between the intensity of the Bfa1-eGFP signal and the interaction of cytoplasmic microtubules with the bud cortex. The observation that under conditions in which microtubule-bud cortex interactions are disrupted Bfa1 localization is impaired indicates that this correlation reflects a causal relationship. Severing of microtubules that interact with the bud cortex leads to a decrease in Bfa1 localization at the dSPB. In cells with mispositioned anaphase spindles, which indicates a failure of microtubules to interact with the bud cortex, Bfa1 is also symmetric. However, there is an important difference in Bfa1 localization between mutants that disrupt microtubule-bud cortex interactions and actin polarity. In cells lacking *KAR9*, both SPBs behave like the mSPB; in cells lacking formins, both SPBs behave like dSPBs. Thus, our data are most consistent with the idea that asymmetry cues determined by actin cytoskeleton polarity are conveyed to SPBs through cytoplasmic microtubules.

Mechanisms of Bfa1 Association with SPBs

The analysis of Bfa1 dynamics provided insights into how Bfa1 association with SPBs is regulated and clarified the role of microtubules in Bfa1 association with SPBs. Although Bfa1 can associate with SPBs in the absence of microtubules, these interactions are transient. In the presence of microtubules that engage in functional interactions with the bud cortex, the residence time of Bfa1 at SPBs is increased. Our results also revealed a difference between the dSPB and the mSPB. On the mSPB, the percentage of signal that was recovered was similar to that seen in nocodazole-treated cells (between 50% and 70%). In contrast, the amount of signal recovered on the dSPB was less than 20%. It is possible that Bfa1 is equally dynamic on both SPBs but the total amount of Bfa1 is rate limiting. In this scenario, the difference in the amount of signal recovery is simply a function of the amount of Bfa1 present on the two SPBs before bleaching and the amount of free Bfa1. However, the difference in signal recovery for the two SPBs remained when we overexpressed Bfa1, arguing against this possibility. We therefore favor the idea that the differences in signal recovery reflect different modes of Bfa1 association with SPBs. We propose that both SPBs are capable of low-affinity recruitment of Bfa1 that is also seen in the absence of functional microtubule-bud cortex interactions. The dSPB is also able to bind Bfa1 with high affinity. This high-affinity binding requires cytoplasmic microtubule-bud cortex interactions. The observation that the percentage of signal recovery on the dSPB in metaphase is the same as that observed on the dSPB in anaphase indicates that the high-affinity interactions occur as soon as cytoplasmic microtubule-bud cortex interactions are established.

The mechanisms creating the two modes of Bfa1 association with SPBs remain to be elucidated. Two types of Bfa1 receptors could exist at SPBs, one low affinity and one high affinity, with the latter depending on microtubule-bud cortex interactions. This does not necessarily mean that two different proteins mediate the two modes of Bfa1 binding. Bud-cortex-interacting microtubules could load factors that convert low-affinity Bfa1 receptors on the dSPB to high-affinity ones. A candidate protein for such a receptor is Nud1, a component of the cytoplasmic face of SPBs (Adams and Kilmartin, 1999). Bfa1 preferentially binds the protein in its phosphorylated form (Gruneberg et al., 2000). Perhaps protein kinases are loaded onto dSPBs in a microtubule-dependent manner, converting Nud1 into a phosphorylated high-affinity Bfa1 receptor. It is also possible that modifications of Bfa1 itself lead to two modes of Bfa1 binding to the SPB. Transport of Bfa1 along bud-cortex-interacting microtubules could convert Bfa1 into a high-affinity form. Bfa1 is a phospho protein, whose phosphorylation sites have been identified (Hu et al., 2001). It will be interesting to determine the localization of Bfa1 mutants in which these sites were mutated to residues that can no longer be phosphorylated or that mimic phosphorylation.

Although phosphorylation could promote the association of Bfa1 with SPBs, the analysis of Bfa1 stability in G1 indicates that, at least, CDKs antagonize rather than promote the stable association of Bfa1 with SPBs. During G1 when CDK levels are low, newly synthesized Bfa1 cannot associate with SPBs. Furthermore, no Bfa1 signal was recovered after photobleaching. These data indicate that during G1 Bfa1 association with SPBs is exceedingly stable. In contrast, 15 min after release from the G1 block, newly synthesized Bfa1 can associate with SPBs, indicating that the protein is dynamic then. It thus appears that CDKs destabilize the Bfa1-SPB interactions. The role of microtubule-bud cortex interactions would then be to antagonize this inhibitory effect.

A Model for How Tem1 Complex Asymmetry Is Generated

We propose the following model for how Bfa1 association with SPBs is controlled in space and time. During G1 the newly born daughter cells carry Bfa1 on their SPBs, whereas mother cells do not. In this cell cycle stage Bfa1 associates with SPBs in a stable manner. Passage through START destabilizes Bfa1 at SPBs and also allows Bfa1 to associate with SPBs in mother cells. As soon as the mitotic spindle has formed, cytoplasmic microtubules start probing and interacting with the cell cortex. Microtubules interacting with the bud cortex facilitate high-affinity interactions of Bfa1 with the SPB they originate from. The factors mediating these high-affinity interactions were transported into or generated in the bud through Cdc42-dependent actin polarization. The actin cytoskeleton, we speculate, helps to generate high-affinity binding determinants or their loading onto microtubules. In cells with mispositioned spindles, in which microtubule-bud cortex interactions are disrupted, the high-affinity interactions are lost and the residence time of Bfa1 on both SPBs is that of mSPBs. It is tempting to speculate that this change in Bfa1 affinity is important for spindle position checkpoint activity. In cells with mispositioned spindles, Tem1 association with SPBs is greatly reduced (D'Aquino et al., 2005; Molk et al., 2004). If Tem1 association with SPBs was important for MEN signaling, reducing the affinity of the Tem1 anchor for SPBs would provide a means to downregulate MEN signaling. In support of this idea is the observation that increasing the residence time of Bfa1 on SPBs leads to spindle position checkpoint defects (Caydasi and Pereira, 2009).

A key question is whether the asymmetric localization of the Tem1 complex is important for MEN signaling. To address this question, Bfa1-Bub2 mutants need to be generated that localize to both SPBs. A mutant version of *BUB2,* in which Bub2 is tagged with nine Myc epitopes at its C terminus, has been shown to localize to both SPBs. This mutant localizes the Tem1 complex to both SPBs but exhibits no apparent defect in an otherwise wild-type background (Fraschini et al., 2006). However, the mutant lacks GAP activity in vitro (Fraschini et al., 2006), indicating that the overall Bub2 structure is altered in the mutant. Cells in which Bfa1 is targeted to both SPBs by fusing it to an integral SPB component are viable (Caydasi and Pereira, 2009), but the effects on cell cycle progression have not been analyzed in detail. Thus, the consequences of targeting a functional Tem1 complex to both SPBs remain unknown. It is however important to note that the asymmetric activation of Tem1 is conserved between the two very distantly related fungi *S. cerevisiae* and *S. pombe*. In fission yeast, which undergoes a morphological symmetrical division, the Tem1 homolog Spg1, though localizing to both SPBs, is activated on only one SPB during anaphase (Sohrmann et al., 1998). Identifying the factors that mediate asymmetry cues from the cortex to the SPB will therefore likely provide important insights into generating centrosome asymmetry in all eukaryotes.

EXPERIMENTAL PROCEDURES

Strains and Plasmids
All strains are derivatives of W303 and are described in Table S1. *BFA1-eGFP*, *BUB2-eGFP*, and *TEM1-eGFP* were generated as described in Sheff and Thorn (2004). *BFA1-mCherry* was generated as described in Snaith et al. (2005). *mCherry-TUB1* was described in Khmelinskii et al. (2007). *TUB1-GFP* was described in Straight et al. (1997). p*CTS1-2xmCherry-SV40NLS* was a gift from Drew Endy's lab. pLP17 CEN plasmid containing *CDC12-GFP* was described in Lippincott and Li (1998).

Immunolocalization Techniques
Indirect in situ immunofluorescence was carried out as described in Visintin et al. (1999). Bfa1-3HA and 3HA-Bub2 were detected using a mouse anti-HA antibody (HA.11, Covance) at a 1:500 dilution. Tem1-13Myc was detected using a mouse anti-Myc antibody (Covance) at a 1:500 dilution. The secondary antibody used was anti-mouse Cy3 (Jackson Immunoresearch) at a 1:2000 dilution. Rat anti-tubulin (Oxford Biotechnology) and anti-rat FITC (Jackson Immunoresearch) antibodies were used at a 1:500 dilution. For imaging of GFP and mCherry-tagged proteins when live-cell microscopy was not used, cells were fixed in 2.5% formaldehyde for 10 min, washed twice with potassium phosphate (pH 6.4), and stored in potassium phosphate (pH 7.4). This was followed by a 10 min 80% ethanol fixation and resuspension in 1 mg/ml 4′,6-diamidino-2-phenylindole (DAPI) or 2 μg/ml Hoechst 3342 (Invitrogen) solution. Phalloidin staining of the cells was performed as described in Cope et al. (1999). Unless otherwise indicated, 100 cells were counted for each time point.

Live Cell Microscopy
Cells were resuspended in synthetic complete medium and analyzed using a Zeiss Observer.Z1 inverted scope. For time-lapse experiments pictures were taken using a Hamamatsu ORCA-ER C4742-80 digital CCD camera and processed with MetaMorph (Molecular Devices) software. This software was also used for the quantification of the fluorescence intensity.

Fluorescence Recovery after Photobleaching
FRAP experiments were carried out using a Micropoint ablation laser system (Photonics Instruments, St. Charles, IL) equipped with a NL100 nitrogen laser and a Micropoint 481 nm laser dye. The area to be photobleached received three pulses of laser (approximate total time = 201 ms) with the attenuation plate set to 12% transmission. Fluorescence recovery was analyzed using the equation: $[F_{inf} - F(t)]/[F_{inf} - F(0)] = 1 - e^{-kt}$, where F_{inf} is the average intensity of the bleached region after maximum recovery, $F(t)$ is the fluorescence intensity at each point, $F(0)$ is the fluorescence immediately after bleaching, k is the rate constant for exponential decay, and t is time. As derived from the previous equation, the slope of the straight line obtained when $1 - ([F_{inf} - F(t)]/[F_{inf} - F(0)])$ is plotted versus time represents the rate constant k. The half recovery time was estimated as $t_{1/2} = \ln 2/k$, whereas the percentage of recovery is given by the equation $\%R = [F_{inf} - F(0)]/[F_{initial} - F(0)]$, where $F_{initial}$ is the initial fluorescence intensity before photobleaching.

Microtubule Severing
Microtubules were severed using the same Micropoint ablation laser system used for FRAP experiments except two pulses of laser (approximate total time = 134 ms) with the attenuation plate set to 31% transmission were used.

SUPPLEMENTAL DATA

Supplemental Data include six figures, six movies, and one table and can be found with this article online at http://www.cell.com/developmental-cell/supplemental/S1534-5807(08)00476-0/.

REFERENCES

Adams, I.R., and Kilmartin, J.V. (1999). Localization of core spindle pole body (SPB) components during SPB duplication in *Saccharomyces cerevisiae*. J. Cell Biol. *145*, 809–823.

Amon, A., Irniger, S., and Nasmyth, K. (1994). Closing the cell cycle circle in yeast: G2 cyclin proteolysis initiated at mitosis persists until the activation of G1 cyclins in the next cycle. Cell *77*, 1037–1050.

Bardin, A.J., Visintin, R., and Amon, A. (2000). A mechanism for coupling exit from mitosis to partitioning of the nucleus. Cell *102*, 21–31.

Benton, B.K., Tinkelenberg, A., Gonzalez, I., and Cross, F.R. (1997). Cla4p, a Saccharomyces cerevisiae Cdc42p-activated kinase involved in cytokinesis, is activated at mitosis. Mol. Cell. Biol. *17*, 5067–5076.

Buttery, S.M., Yoshida, S., and Pellman, D. (2007). Yeast formins Bni1 and Bnr1 utilize different modes of cortical interaction during the assembly of actin cables. Mol. Biol. Cell *18*, 1826–1838.

Carvalho, P., and Pellman, D. (2004). Mitotic spindle: laser microsurgery in yeast cells. Curr. Biol. *14*, R748–R750.

Caydasi, A.K., and Pereira, G. (2009). Spindle alignment regulates the dynamic association of checkpoint proteins with yeast spindle pole bodies. Dev. Cell *16*, this issue, 146–156.

Cope, M.J., Yang, S., Shang, C., and Drubin, D.G. (1999). Novel protein kinases Ark1p and Prk1p associate with and regulate the cortical actin cytoskeleton in budding yeast. J. Cell Biol. *144*, 1203–1218.

Cvrckova, F., De Virgilio, C., Manser, E., Pringle, J.R., and Nasmyth, K. (1995). Ste20-like protein kinases are required for normal localization of cell growth and for cytokinesis in budding yeast. Genes Dev. *9*, 1817–1830.

D'Aquino, K.E., Monje-Casas, F., Paulson, J., Reiser, V., Charles, G.M., Lai, L., Shokat, K.M., and Amon, A. (2005). The protein kinase Kin4 inhibits exit from mitosis in response to spindle position defects. Mol. Cell 19, 223–234.

Evangelista, M., Blundell, K., Longtine, M.S., Chow, C.J., Adames, N., Pringle, J.R., Peter, M., and Boone, C. (1997). Bni1p, a yeast formin linking Cdc42p and the actin cytoskeleton during polarized morphogenesis. Science 276, 118–122.

Evangelista, M., Pruyne, D., Amberg, D.C., Boone, C., and Bretscher, A. (2002). Formins direct Arp2/3-independent actin filament assembly to polarize cell growth in yeast. Nat. Cell Biol. 4, 32–41.

Faty, M., Fink, M., and Barral, Y. (2002). Septins: a ring to part mother and daughter. Curr. Genet. 41, 123–131.

Fraschini, R., D'Ambrosio, C., Venturetti, M., Lucchini, G., and Piatti, S. (2006). Disappearance of the budding yeast Bub2-Bfa1 complex from the mother-bound spindle pole contributes to mitotic exit. J. Cell Biol. 172, 335–346.

Fujiwara, T., Tanaka, K., Mino, A., Kikyo, M., Takahashi, K., Shimizu, K., and Takai, Y. (1998). Rho1p-Bni1p-Spa2p interactions: implication in localization of Bni1p at the bud site and regulation of the actin cytoskeleton in Saccharomyces cerevisiae. Mol. Biol. Cell 9, 1221–1233.

Gruneberg, U., Campbell, K., Simpson, C., Grindlay, J., and Schiebel, E. (2000). Nud1p links astral microtubule organization and the control of exit from mitosis. EMBO J. 19, 6475–6488.

Hu, F., Wang, Y., Liu, D., Li, Y., Qin, J., and Elledge, S.J. (2001). Regulation of the Bub2/Bfa1 GAP complex by Cdc5 and cell cycle checkpoints. Cell 107, 655–665.

Imamura, H., Tanaka, K., Hihara, T., Umikawa, M., Kamei, T., Takahashi, K., Sasaki, T., and Takai, Y. (1997). Bni1p and Bnr1p: downstream targets of the Rho family small G-proteins which interact with profilin and regulate actin cytoskeleton in Saccharomyces cerevisiae. EMBO J. 16, 2745–2755.

Jeong, J.W., Kim, D.H., Choi, S.Y., and Kim, H.B. (2001). Characterization of the CDC10 product and the timing of events at the budding site of Saccharomyces cerevisiae. Mol. Cells 12, 77–83.

Khmelinskii, A., Lawrence, C., Roostalu, J., and Schiebel, E. (2007). Cdc14-regulated midzone assembly controls anaphase B. J. Cell Biol. 177, 981–993.

Kohno, H., Tanaka, K., Mino, A., Umikawa, M., Imamura, H., Fujiwara, T., Fujita, Y., Hotta, K., Qadota, H., Watanabe, T., et al. (1996). Bni1p implicated in cytoskeletal control is a putative target of Rho1p small GTP binding protein in Saccharomyces cerevisiae. EMBO J. 15, 6060–6068.

Kosco, K.A., Pearson, C.G., Maddox, P.S., Wang, P.J., Adams, I.R., Salmon, E.D., Bloom, K., and Huffaker, T.C. (2001). Control of microtubule dynamics by Stu2p is essential for spindle orientation and metaphase chromosome alignment in yeast. Mol. Biol. Cell 12, 2870–2880.

Leberer, E., Wu, C., Leeuw, T., Fourest-Lieuvin, A., Segall, J.E., and Thomas, D.Y. (1997). Functional characterization of the Cdc42p binding domain of yeast Ste20p protein kinase. EMBO J. 16, 83–97.

Li, R. (1999). Bifurcation of the mitotic checkpoint pathway in budding yeast. Proc. Natl. Acad. Sci. USA 96, 4989–4994.

Lippincott, J., and Li, R. (1998). Dual function of Cyk2, a cdc15/PSTPIP family protein, in regulating actomyosin ring dynamics and septin distribution. J. Cell Biol. 143, 1947–1960.

Longtine, M.S., and Bi, E. (2003). Regulation of septin organization and function in yeast. Trends Cell Biol. 13, 403–409.

Maekawa, H., and Schiebel, E. (2004). Cdk1-Clb4 controls the interaction of astral microtubule plus ends with subdomains of the daughter cell cortex. Genes Dev. 18, 1709–1724.

Maekawa, H., Usui, T., Knop, M., and Schiebel, E. (2003). Yeast Cdk1 translocates to the plus end of cytoplasmic microtubules to regulate bud cortex interactions. EMBO J. 22, 438–449.

McCollum, D., and Gould, K.L. (2001). Timing is everything: regulation of mitotic exit and cytokinesis by the MEN and SIN. Trends Cell Biol. 11, 89–95.

McMillan, J.N., Sia, R.A., and Lew, D.J. (1998). A morphogenesis checkpoint monitors the actin cytoskeleton in yeast. J. Cell Biol. 142, 1487–1499.

Menssen, R., Neutzner, A., and Seufert, W. (2001). Asymmetric spindle pole localization of yeast Cdc15 kinase links mitotic exit and cytokinesis. Curr. Biol. 11, 345–350.

Molk, J.N., Schuyler, S.C., Liu, J.Y., Evans, J.G., Salmon, E.D., Pellman, D., and Bloom, K. (2004). The differential roles of budding yeast Tem1p, Cdc15p, and Bub2p protein dynamics in mitotic exit. Mol. Biol. Cell 15, 1519–1532.

Moseley, J.B., and Goode, B.L. (2005). Differential activities and regulation of Saccharomyces cerevisiae formin proteins Bni1 and Bnr1 by Bud6. J. Biol. Chem. 280, 28023–28033.

Norden, C., Liakopoulos, D., and Barral, Y. (2004). Dissection of septin actin interactions using actin overexpression in Saccharomyces cerevisiae. Mol. Microbiol. 53, 469–483.

Ozaki-Kuroda, K., Yamamoto, Y., Nohara, H., Kinoshita, M., Fujiwara, T., Irie, K., and Takai, Y. (2001). Dynamic localization and function of Bni1p at the sites of directed growth in Saccharomyces cerevisiae. Mol. Cell. Biol. 21, 827–839.

Park, H.O., Bi, E., Pringle, J.R., and Herskowitz, I. (1997). Two active states of the Ras-related Bud1/Rsr1 protein bind to different effectors to determine yeast cell polarity. Proc. Natl. Acad. Sci. USA 94, 4463–4468.

Park, H.O., Sanson, A., and Herskowitz, I. (1999). Localization of Bud2p, a GTPase-activating protein necessary for programming cell polarity in yeast to the presumptive bud site. Genes Dev. 13, 1912–1917.

Pereira, G., and Schiebel, E. (2005). Kin4 kinase delays mitotic exit in response to spindle alignment defects. Mol. Cell 19, 209–221.

Pereira, G., Hofken, T., Grindlay, J., Manson, C., and Schiebel, E. (2000). The Bub2p spindle checkpoint links nuclear migration with mitotic exit. Mol. Cell 6, 1–10.

Pereira, G., Tanaka, T.U., Nasmyth, K., and Schiebel, E. (2001). Modes of spindle pole body inheritance and segregation of the Bfa1p-Bub2p checkpoint protein complex. EMBO J. 20, 6359–6370.

Peter, M., Neiman, A.M., Park, H.O., van Lohuizen, M., and Herskowitz, I. (1996). Functional analysis of the interaction between the small GTP binding protein Cdc42 and the Ste20 protein kinase in yeast. EMBO J. 15, 7046–7059.

Pruyne, D., and Bretscher, A. (2000a). Polarization of cell growth in yeast. I. Establishment and maintenance of polarity states. J. Cell Sci. 113, 365–375.

Pruyne, D., and Bretscher, A. (2000b). Polarization of cell growth in yeast. II. The role of the cortical actin cytoskeleton. J. Cell Sci. 113, 571–585.

Sagot, I., Klee, S.K., and Pellman, D. (2002). Yeast formins regulate cell polarity by controlling the assembly of actin cables. Nat. Cell Biol. 4, 42–50.

Seshan, A., and Amon, A. (2004). Linked for life: temporal and spatial coordination of late mitotic events. Curr. Opin. Cell Biol. 16, 41–48.

Sheff, M.A., and Thorn, K.S. (2004). Optimized cassettes for fluorescent protein tagging in Saccharomyces cerevisiae. Yeast 21, 661–670.

Sheu, Y.J., Santos, B., Fortin, N., Costigan, C., and Snyder, M. (1998). Spa2p interacts with cell polarity proteins and signaling components involved in yeast cell morphogenesis. Mol. Cell. Biol. 18, 4053–4069.

Shou, W., Seol, J.H., Shevchenko, A., Baskerville, C., Moazed, D., Chen, Z.W., Jang, J., Charbonneau, H., and Deshaies, R.J. (1999). Exit from mitosis is triggered by Tem1-dependent release of the protein phosphatase Cdc14 from nucleolar RENT complex. Cell 97, 233–244.

Snaith, H.A., Samejima, I., and Sawin, K.E. (2005). Multistep and multimode cortical anchoring of tea1p at cell tips in fission yeast. EMBO J. 24, 3690–3699.

Sohrmann, M., Schmidt, S., Hagan, I., and Simanis, V. (1998). Asymmetric segregation on spindle poles of the Schizosaccharomyces pombe septum-inducing protein kinase Cdc7p. Genes Dev. 12, 84–94.

Stegmeier, F., and Amon, A. (2004). Closing mitosis: the functions of the Cdc14 phosphatase and its regulation. Annu. Rev. Genet. 38, 203–232.

Straight, A.F., Marshall, W.F., Sedat, J.W., and Murray, A.W. (1997). Mitosis in living budding yeast: anaphase A but no metaphase plate. Science 277, 574–578.

Theesfeld, C.L., Irazoqui, J.E., Bloom, K., and Lew, D.J. (1999). The role of actin in spindle orientation changes during the Saccharomyces cerevisiae cell cycle. J. Cell Biol. 146, 1019–1032.

Vallen, E.A., Caviston, J., and Bi, E. (2000). Roles of Hof1p, Bni1p, Bnr1p, and myo1p in cytokinesis in *Saccharomyces cerevisiae*. Mol. Biol. Cell *11*, 593–611.

Visintin, R., Craig, K., Hwang, E.S., Prinz, S., Tyers, M., and Amon, A. (1998). The phosphatase Cdc14 triggers mitotic exit by reversal of Cdk-dependent phosphorylation. Mol. Cell *2*, 709–718.

Visintin, R., Hwang, E.S., and Amon, A. (1999). Cfi1 prevents premature exit from mitosis by anchoring Cdc14 phosphatase in the nucleolus. Nature *398*, 818–823.

Vojtek, A.B., and Cooper, J.A. (1995). Rho family members: activators of MAP kinase cascades. Cell *82*, 527–529.

Yeh, E., Yang, C., Chin, E., Maddox, P., Salmon, E.D., Lew, D.J., and Bloom, K. (2000). Dynamic positioning of mitotic spindles in yeast: role of microtubule motors and cortical determinants. Mol. Biol. Cell *11*, 3949–3961.

Zheng, Y., Bender, A., and Cerione, R.A. (1995). Interactions among proteins involved in bud-site selection and bud-site assembly in *Saccharomyces cerevisiae*. J. Biol. Chem. *270*, 626–630.